RSC Advances

ROYAL SOCIETY OF CHEMISTRY

www.rsc.org/advances

(RSC Advances)

Flexible, nonenzymatic glucose biosensor based on Ni-coordinated, vertically aligned carbon nanotube arrays

Wan-Sun Kim[1,2], Je-Hwang Ryu[1], Kyu-Chang Park[3], Gi-Ja Lee[1,2*] and Hun-Kuk Park[1,2*]

[1]Department of Biomedical Engineering & Healthcare Industry Research Institute, College of Medicine, Kyung Hee University, Seoul 130-701, Korea

[2]Department of Medical Engineering, Kyung Hee University Graduate School, Seoul 130-701, Korea

[3]Department of Information Display and Advanced Display Research Center, Kyung Hee University, Seoul 130-701, Korea

Corresponding author:

Hun-Kuk Park, M.D., Ph.D. & Gi-Ja Lee, Ph.D.

Department of Biomedical Engineering

College of Medicine, Kyung Hee University

1 Hoegi-dong, Dongdaemun-gu, Seoul 130-701, Republic of Korea

Tel.: +82 2 961 0290; Fax: +82 2 6008 5535

E-mail address: sigmoidus@khu.ac.kr, gjlee@khu.ac.kr

ABSTRACT

We evaluated the use of flexible biosensors based on Ni-coordinated, vertically aligned carbon nanotubes on a flexible graphite substrate (Ni/VCNTs/G) for nonenzymatic electrochemical detection of glucose. The Ni/VCNTs/G electrodes were fabricated by a simple process of radiofrequency sputtering and plasma-enhanced chemical vapour deposition. We performed cyclic voltammetry and chronoamperometry for electrochemical characterization of the Ni/VCNTs/G electrodes. In addition, we examined the effect of mechanical bending on their sensing performance. The electrodes exhibited enhanced electrocatalytic activity toward the oxidation of glucose in alkaline solution compared to the bare graphite, Ni particles, and vertically aligned CNTs on graphite. They also exhibited a sensitivity of 950.6 $\mu A \cdot mM^{-1} \cdot cm^{-2}$ to glucose with a linear range of 0.05 to 1.0 mM and a detection limit of 30 μM. In particular, there was no significant change in the amperometric signal of the electrodes, showing a sensitivity of 910.7 $\mu A \cdot mM^{-1} \cdot cm^{-2}$ (only a 4% decrease in the initial response) after the 200^{th} bending. Moreover, the Ni/VCNTs/G electrodes were less sensitive to common interfering species such as ascorbic acid, uric acid, galactose, and xylose than to glucose. In sum, our Ni/VCNTs/G electrodes exhibited enhanced electrocatalytic activity, good sensitivity, a fast response, high selectivity, and excellent mechanical stability. Therefore, we expect that our flexible, nonenzymatic glucose biosensor based on this electrode will open exciting opportunities for wearable, real-time, and/or on-site applications in fields ranging from clinical analysis to industry.

Introduction

Flexible technology has been highlighted in the fields of electronic circuits, displays, radio-frequency identification, and appliances over the past several decades.[1–4] In particular, flexible biosensors, which make biosensors more portable and biocompatible, have great potential in health care, sports, and defence applications.[5–8] It is critical to fabricate flexible biosensors with not only a flexible electrode material, but also a flexible substrate for application to curved surfaces such as the human body. Many studies have suggested the use of a combination of carbon materials (e.g., carbon nanotubes [CNTs] and graphene) or conductive polymers with flexible substrates such as polydimethyl siloxane, polyethylene terephthalate, polyimide, and transparent conductive film.[9–14] However, because conductive materials must be fixed or coated onto flexible substrates, the resulting devices might lack reliability and robustness for biosensor applications.

CNTs have been widely utilized as an electrode material for highly sensitive biosensors because of their high surface-to-volume ratio, excellent electrical conductivity, rapid electrode kinetics, chemical stability, and good mechanical properties.[15–17] We previously reported new conductive, flexible, all-carbon electrodes consisting of CNTs on a flexible graphite foil utilizing plasma-enhanced chemical vapour deposition (PECVD).[18] The combination of CNTs with graphite produces hybrid electrodes with superior characteristics including effective electron transfer and a larger surface area for high sensitivity and mechanical flexibility. Therefore, we expected that they could be utilized as highly stable, cost-effective flexible electrochemical biosensors with outstanding performance.

Rapid and reliable glucose monitoring is important in the diagnosis and management of

diabetes mellitus, the treatment of industrial waste water, and the preparation of food. Although conventional glucose sensors based on glucose oxidase show very high sensitivity and selectivity to glucose, they have drawbacks including their high cost, complicated immobilization process, and poor stability in response to changes in environmental conditions such as temperature, pH, humidity, and toxic chemicals because of the intrinsic nature of enzymes. To solve this problem, nonenzymatic glucose sensors that can directly oxidize glucose on the electrode surface have been developed. These sensors utilize electrocatalyst including metals (e.g., Cu, Ni, Pt), metal oxides (e.g., CuO, Fe_3O_4, Mn_xO_y), alloys (e.g., PtAu, PtPd), and complexes bound to carbon-based materials with excellent electrical properties.[9, 10, 19–26] Among them, Ni-based nanomaterials have shown excellent electrocatalytic capability for glucose detection. Modified electrodes with variously shaped Ni-based nanomaterials have been explored for glucose detection utilizing the redox reaction of $Ni(OH)_2$/NiOOH.[21,27,28] However, the preparation process for an electrocatalyst requires a long period of time and is complex because of the need to perform wet chemical synthesis. Moreover, the catalysts must be combined with other flexible substrates or electrode materials, further increasing the complexity of this process. To date, most nonenzymatic glucose biosensors have been fabricated on a rigid electrode such as metal or glassy carbon substrate, which is vulnerable to mechanical stress including bending and tensile or compressive strain.[20–26, 28]

Therefore, in this study, we fabricated Ni-coordinated, vertically aligned CNTs that were directly grown on a flexible graphite substrate (Ni/VCNTs/G) through simple fabrication without a wet chemical process. We also investigated the performance of these Ni/VCNTs/Gs, including their sensitivity, selectivity, and reproducibility as a flexible nonenzymatic glucose sensor. In particular, we examined the change in their sensitivity to glucose after the bending test.

EXPERIMENTAL SECTION

A. Materials

D-(+)-glucose, ascorbic acid (AA), galactose (GA), uric acid (UA), xylose (XY), $K_3[Fe(CN)_6]$, and human serum (4.89 mM, H4522) were purchased from Sigma Aldrich (St. Louis, MO, USA). NaOH and KCl were obtained from Duksan Pure Chemicals Co., Ltd. (Ansan, Gyeonggi, Korea) and Junsei Chemical Co., Ltd. (Chuo-ku, Tokyo, Japan), respectively. All aqueous solutions were prepared using distilled water with a resistivity of 18.3 $M\Omega \cdot cm^{-1}$. The glucose stock solution was allowed to mutarotase overnight before use. A flexible graphite foil was used (GoodFellow, Coraopolis, PA, USA); this foil has a 0.125 mm thickness and 99.8% purity with flexibility. Nickel (99.9999% purity) for sputtering was purchased from Kojundo Chemical Lab. (Sakado-shi, Saitama, Japan).

B. Preparation of VCNTs/G

The VCNTs were grown directly on flexible graphite foil as previously described.[18] Fig. 1A shows a schematic diagram of the fabrication process. In short, the Ni layer as the catalyst material for CNTs was deposited on the flexible bare graphite foil by radio frequency (RF) sputtering at a power of 40 W for 3 min under a pressure of 1 mTorr Ar ambient. The foil was heated for 30 min at 600 °C under 0.3 Torr Ar ambient to form the Ni particles. The VCNTs were grown on the granulated Ni particles on graphite foil utilizing a direct-current PECVD (dc-PECVD) system. The power was 120 W, bias was –700 V, and spacing between the two electrodes was 30 mm. C_2H_2 and NH_3 gases were used for CNT growth at a pressure of 2 Torr

for 20 min and flow rates of 40 and 60 sccm, respectively. The growth temperature was maintained at 700 °C.

C. Fabrication of Ni/VCNTs/G

Because the granulated Ni for the growth of CNT was surrounded by the carbon layers,[18] we performed additionally RF sputtering to introduce Ni as an electrocatalyst for the detection of glucose. The conditions were identical to those used to deposit the Ni layer onto graphite foil with the exception of a deposition time of 20 min. No wet processes were carried out during the entire manufacturing process because we used RF sputtering and the PECVD method for both Ni deposition and CNT growth. Fig. 1B shows a photograph of a flexible Ni/VCNTs/G electrode. Our Ni/VCNTs/G electrodes can be easily modified into the desired size or shape using a scissors or knife, as shown in Fig. 1C. To perform electrochemical measurements, we cut the electrodes to a length of 20 mm and width of 3 mm. Then the electrodes were insulated with nail enamel excluding the active area of 3×3 mm^2.

D. Characterization and electrochemical measurements

The morphologies of the as-prepared Ni/VCNTs/G were characterized using a field emission scanning electron microscope (FE-SEM; S-4700, Hitachi, Tokyo, Japan). An energy-dispersive X-ray spectroscope (EDX; 7200-H, HORIBA, Northampton, England) was used to examine the elemental composition of the synthesized products. The electrochemical measurements were carried out with an electrochemical analyzer (PARSTAT 2263; Princeton Applied Research, TN, USA) in a conventional three-electrode cell. The modified electrodes were used as working electrodes. An Ag/AgCl (sat. KCl) and a platinum wire were employed as

reference and counter electrode, respectively. All electrochemical measurements were carried out at room temperature. A 0.1 M NaOH solution was used as supporting electrolyte. All samples underwent 10 cycles from –1.2 to 0.8 V in the 0.1 M KCl solution for cleaning before conducting measurements.

To understand the amperometric response of the flexible Ni/VCNTs/G electrodes when subjected to mechanical bending, their current responses were measured after being bent 200 times using continuous rolling cycles with an approximately 5 mm radius of curvature.

RESULTS AND DISCUSSION

A. Fabrication and characterization of Ni/VCNTs/Gs

Because VCNTs have excellent nanotube alignment, a highly effective surface area, and good electrical and thermal conductivity, they can be utilized in many applications such as field emission displays, polymer fillers, and in particular, chemical and biological sensors.[29] Their excellent mechanical conformability enables them to be incorporated as flexible elements into future flexible devices.[30] We previously suggested the use of VCNTs on a flexible graphite foil for flexible electrochemical applications in which the bond between the graphite substrate and the CNTs is strong enough to withstand any mechanical stress.[18] Therefore, in this study, we incorporated Ni, which showed better performance in the electro-oxidation of glucose than did other metallic electrodes in Ni/VCNTs/G for use as a flexible glucose biosensor.

Fig. 2 illustrates the morphology and elemental composition of the VCNTs/G and Ni/VCNTs/G, respectively. As shown in Fig. 2A, the CNTs obtained using the PECVD method

for 20 min were vertically grown on graphite foil about 2 μm in length and 10 to 150 nm in diameter according to the size of the granulated Ni. Because the VCNTs/G was densely and uniformly packed on graphite foil, the surface area in a limited substrate could be maximized. The morphology of the as-prepared Ni/VCNTs/G is depicted in Fig. 2B. The VCNTs were evenly covered with the Ni layer as electrocatalyst of glucose detection. The thickness of the Ni layer on the VCNTs/G was about 20 nm after a deposition time of 20 min using RF sputtering. From the EDX spectrum shown in Fig. 2C and D, we confirmed that the VCNTs/G consisted only of carbon and that the Ni/VCNTs/G electrodes were composed of both Ni and carbon at ratios of 25 and 75 wt%, respectively.

Prior to testing the sensing performance of Ni/VCNTs/G for glucose, we compared the electrochemical behavior of four kinds of electrodes including bare graphite foil, Ni nanoparticles on graphite foil, VCNTs/G, and Ni/VCNTs/G in 0.1 M NaOH solution at a scan rate of 50 $mV \cdot s^{-1}$. The Ni nanoparticles on graphite foil were made by RF sputtering during 20 min and granulated for 30 min at 600 °C. As shown in curves a and c of Fig. 3A, there were no reaction peak currents in both the bare graphite foil and VCNTs/G electrodes which were only consisted with carbon. This means that these two electrodes were not involved in the redox reaction in the potential range from + 0.10 to + 0.60 V. Although the Ni nanoparticles on graphite foil showed a small, broad redox peak (curve b of Fig. 3A, inset), the anodic and cathodic peak currents in the Ni/VCNTs/G electrode (curve d) were stronger than those in the Ni nanoparticles on graphite foil (curve b). A pair of well-defined redox peaks might be attributed to Ni(II)/Ni(III) redox coupling in the alkaline solution, as previously reported in literatures[21,31]:

$$Ni + 2OH^- - 2e^- \rightarrow Ni(OH)_2$$

$$Ni(OH)_2 + OH^- - e^- \rightarrow NiO(OH) + H_2O$$

It seems that a strong peak current on the Ni/VCNTs/G electrode resulted from its larger surface area of VCNTs and sufficiently incorporated Ni by a synergic effect. Therefore, it appears that the Ni/VCNTs/G electrodes would be effective for the direct oxidation of glucose on their surface. The electrochemical active surface area of the Ni/VCNTs/G was estimated using Randles–Sevcik equation employing $K_3[Fe(CN)_6]$ as a model redox mediator, as shown in Fig. S1 (ESI). As a result, the active surface area of Ni/VCNTs/G was 0.2 cm^2.

Fig. 3B represents the CVs of the Ni/VCNTs/G electrode in a solution of 0.1 M NaOH at different scan rates (10 – 200 $mV \cdot s^{-1}$). Both the anodic and cathodic peak currents were linearly proportional to the square root of the scan rate (R^2 for the anodic and cathodic peak was 0.9966 and 0.9945, respectively), demonstrated the electrochemical process was typically diffusion-controlled. Because no obvious change in peak current was found during 10 consecutive CV curves at a scan rate of 50 $mV \cdot s^{-1}$, the Ni/VCNTs/G electrode seemed to be stable (data not shown).

B. Electrocatalytic determination of glucose

To investigate electrocatalytic glucose oxidation activity, we carried out cyclic voltammetry of the Ni/VCNTs/G electrode in 0.1 M NaOH solutions with and without 2 mM glucose. As shown in Fig. 4A, the anodic peak current was substantially higher and the cathodic peak current was lower in the presence of glucose than in the absence of glucose. This indicates that Ni/VCNTs/G has excellent electrocatalytic activity for the direct oxidation of glucose, consistent with previous reports.[21,28]

$$Ni(OH)_2 + OH^- \rightarrow NiO(OH) + H_2O + e^-$$

$$NiO(OH) + \text{glucose} \rightarrow Ni(OH)_2 + \text{glucolactone}$$

Moreover, the anodic peak potential shifts to a more positive value with the addition of glucose, which might be attributed to the diffusion limitation at the electrode surface. As shown in Fig. 3B, Ni(II)/Ni(III) redox reaction is a diffusion-controlled process. Initially, a short dynamic balance could be reached between Ni(III), Ni(II) and hydroxyl ions at the anodic peak potential. The presence of glucose consumed some of the Ni(III). Subsequently, Ni(II) should react with the hydroxyl ions at the interface of the electrode and solution to reach a new balance. Due to the existence of a hydroxyl concentration polarization, a more positive potential was needed for the formation of Ni(III).[32]

For amperometric glucose sensing, we measured the current response of Ni/VCNTs/G to successive injection of glucose in a 0.1 M NaOH solution at an applied potential of + 0.50 V versus Ag/AgCl. Fig. 4B shows the amperometric response of the Ni/VCNTs/G electrode before the 200th bending by successive addition of 0.1 mM glucose. Because the Ni/VCNTs/G electrode quickly produced a steady-state current within 2 sec upon each addition of glucose, we expected that it could be utilized as a rapid and sensitive glucose sensor. We injected a low concentration of glucose to estimate the limit of detection, which was estimated to be 30 μM at a signal-to-noise ratio of 3, as shown in the inset of Fig. 4B.

The influence of mechanical stress on sensor performance must be evaluated for the sensor to be utilized in real life as a flexible biosensor. We examined the effect of mechanical bending on the sensing performance of Ni/VCNTs/G electrodes. Fig. 4C shows the corresponding calibration plot of the response to glucose at a concentration of 50 μM to 1.3 mM by bending cycles. The Ni/VCNTs/G electrode showed a linear correlation with the glucose concentration from 50 μM to 1.0 mM with a correlation

coefficient of 0.999 and sensitivity of 950.6 $\mu A \cdot mM^{-1} \cdot cm^{-2}$. After the 200th bending, there was no significant change in the amperometric signal of the Ni/VCNTs/G electrode, showing a sensitivity of 910.7 $\mu A \cdot mM^{-1} \cdot cm^{-2}$ (only a 4% decrease in the initial response). This may have resulted from the excellent mechanical stability of the flexible Ni/VCNTs/G electrode, in which Ni/VCNTs had good adhesion to the flexible graphite.[18]

The performance of our flexible Ni/VCNTs/G biosensor is compared to that of other flexible glucose sensors in Table 1. Our sensor exhibited excellent performance in terms of sensitivity, response time, and linear range. Its high sensitivity and rapid response might be attributed to the excellent electrocatalytic activity by well-dispersed Ni and the rapid electron transfer of VCNTs. In particular, sensor performance was well maintained even after 200 bending cycles due to its remarkable mechanical stability and flexibility.

C. Selectivity, reproducibility, and stability of Ni/VCNTs/G

Selectivity is one of the most important attributes of a biosensor. In particular, it is very important to use a nonenzymatic glucose biosensor without enzymes such as glucose oxidase, which reacts only to glucose. In general, some oxidizable compounds including AA, GA, UA, and XY can interfere with the electrochemical signal of glucose.[19,21] The physiological level of glucose in normal serum is 3 – 8 mM and the levels of these interfering species are no more than 0.1 mM, though a ratio between glucose and interferences is even higher in food samples. To examine the selectivity of our Ni/VCNTs/G electrode, we compared the current response of 5 mM glucose with that of the normal physiological level of 0.1 mM AA, GA, UA, and XY. As shown in Fig. 5, the interference currents by AA, GA, UA, and XY were negligible, unlike the strong response by glucose. The current response by AA, GA, XY, and UA was only 2.6%, 2.6%,

2.1%, and 0.5%, respectively. These results suggest that the Ni/VCNTs/G electrode has high selectivity for the detection of glucose.

The reproducibility of the Ni/VCNTs/G electrode was also investigated by evaluating the amperometric responses to 0.1 mM glucose in a 0.1 M NaOH solution utilizing five electrodes on different fabrication dates. Because the relative standard deviation of our electrode was 3.4%, the Ni/VCNTs/G electrode was highly reproducible.

The stability of our Ni/VCNTs/G electrode was examined by current responses to 0.1 mM glucose after 60 days of storage in air under ambient conditions. There was no significant change in the current response for glucose (about 96% of initial response), indicating that the Ni/VCNTs/G electrode has high stability.

D. Real sample analysis

To verify the reliability of the Ni/VCNTs/G for routine analysis, the sensor was applied to determine glucose in human serum samples. Human serum sample with the known concentration of glucose (4.89 mM)[35,36] was injected into 10 mL of 0.1 M NaOH solution at an applied potential of + 0.50 V. The recovery of glucose was testified using standard addition method with three times addition of pure glucose to the solutions containing the serum samples. As shown in Table S1 (ESI), the results represented that the sensor gave recoveries in the range of 98.3 – 101.2%. Therefore our Ni/VCNTs/G electrodes have great potential for real application like clinical sample analysis.

CONCLUSIONS

In summary, we have introduced a new, flexible, and sensitive nonenzymatic glucose sensor based on a Ni/VCNTs/G electrode that was simply fabricated by RF sputtering and PECVD without complex or wet processes. The flexible Ni/VCNTs/G electrode, which exhibits reliable adhesion between Ni/VCNTs and graphite foil, showed good sensitivity (950.6 $\mu A \cdot mM^{-1} \cdot cm^{-2}$), a rapid response (< 2 sec), high selectivity, and excellent mechanical stability that allowed for maintenance of the initial sensitivity (only a 4% decrease in the initial response). Therefore, this electrode for nonenzymatic glucose detection holds great promise, especially for portable and wearable glucose-monitoring applications.

Acknowledgments

This work was supported by the industrial strategic technology development program funded by the Ministry of Trade, Industry & Energy (Grant No. 10037379 and 10049035).

Notes and reference

1. A. C. Siegel, S. T. Phillips, M. D. Dickey, N. Lu, Z. Suo, and G. M. Whitesides, *Adv. Funct. Mater.*, 2010, **20**, 28–35.
2. M.-C. Choi, Y. Kim, and C.-S. Ha, *Prog. Polym. Sci.*, 2008, **33**, 581–630.
3. L. Zhou, A. Wanga, S.-C. Wu, J. Sun, S. Park, and T. N. Jackson, *Appl. Phys. Lett.*, 2006, **88**, 083502.
4. B. K. C. Kjellander, W. T. T. Smaal, K. Myny, J. Genoe, W. Dehaene, P. Heremans, and G. H. Gelinck, *Org. Electron.*, 2013, **14**, 768–774.
5. R. Paradiso, G. Loriga, and N. Taccini, *IEEE Trans. Inf. Technol. Biomed.*, 2005, **9**, 337–344.
6. R. G. Haahr, S. B. Duun, M. H. Toft, B. Belhage, J. Larsen, K. Birkelund, and E. V Thomsen, *IEEE Trans. Biomed. Circuits Syst.*, 2012, **6**, 45–53.
7. C.-Y. Chen, C.-L. Chang, T.-F. Chien, and C.-H. Luo, *Sensors Actuators A Phys.*, 2013, **203**, 20–28.
8. M. Ermes, J. Pärkka, J. Mantyjarvi, and I. Korhonen, *IEEE Trans. Inf. Technol. Biomed.*, 2008, **12**, 20–26.
9. P. Si, X.-C. Dong, P. Chen, and D.-H. Kim, *J. Mater. Chem. B*, 2013, **1**, 110-115.
10. F. Xiao, Y. Li, H. Gao, S. Ge, and H. Duan, *Biosens. Bioelectron.*, 2013, **41**, 417–423.
11. H. Kudo, T. Sawada, E. Kazawa, H. Yoshida, Y. Iwasaki, and K. Mitsubayashi, *Biosens. Bioelectron.*, 2006, **22**, 558–562.
12. D. Pradhan, F. Niroui, and K. T. Leung, *ACS Appl. Mater. Interfaces*, 2010, **2**, 2409–2412.

13. X. B. Yan, X. J. Chen, B. K. Tay, and K. a. Khor, *Electrochem. commun.*, 2007, **9**, 1269–1275.

14. S. Iguchi, H. Kudo, T. Saito, M. Ogawa, H. Saito, K. Otsuka, A. Funakubo, and K. Mitsubayashi, *Biomed. Microdevices*, 2007, **9**, 603–609.

15. J. Wang and M. Musameh, *Anal. Chem.*, 2003, **75**, 2075–2079.

16. Y. Lin, F. Lu, Y. Tu, and Z. Ren, *Nano Lett.*, 2004, **4**, 191–195.

17. J. Wang, M. Musameh, and Y. Lin, *J. Am. Chem. Soc.*, 2003, **125**, 2408–2409.

18. J.-H. Ryu, G.-J. Lee, W.-S. Kim, H.-E. Lim, M. Mativenga, K.-C. Park, and H.-K. Park, *Materials (Basel).*, 2014, **7**, 1975–1983.

19. J. Zhao, L. Wei, C. Peng, Y. Su, Z. Yang, L. Zhang, H. Wei, and Y. Zhang, *Biosens. Bioelectron.*, 2013, **47**, 86–91.

20. J. Huang, Z. Dong, Y. Li, J. Li, J. Wang, H. Yang, S. Li, S. Guo, J. Jin, and R. Li, *Sensors Actuators B Chem.*, 2013, **182**, 618–624.

21. H. Nie, Z. Yao, X. Zhou, Z. Yang, and S. Huang, *Biosens. Bioelectron.*, 2011, **30**, 28–34.

22. Z. Wen, S. Ci, and J. Li, *J. Phys. Chem. C*, 2009, **113**, 13482–13487.

23. L.-C. Jiang and W.-D. Zhang, *Biosens. Bioelectron.*, 2010, **25**, 1402–1407.

24. S. Masoomi-Godarzi, a. a. Khodadadi, M. Vesali-Naseh, and Y. Mortazavi, *J. Electrochem. Soc.*, 2014, **161**, B19–B25.

25. J. Chen, W.-D. Zhang, and J.-S. Ye, *Electrochem. commun.*, 2008, **10**, 1268–1271.

26. K.-J. Chen, C.-F. Lee, J. Rick, S.-H. Wang, C.-C. Liu, and B.-J. Hwang, *Biosens. Bioelectron.*, 2012, **33**, 75–81.

27. A. Safavi, N. Maleki, and E. Farjami, *Biosens. Bioelectron.*, 2009, **24**, 1655–1660.

28. M. Shamsipur, M. Najafi, and M.-R. M. Hosseini, *Bioelectrochemistry*, 2010, **77**, 120–124.

29. E. Van Hooijdonk, C. Bittencourt, R. Snyders, and J.-F. Colomer, *Beilstein J. Nanotechnol.*, 2013, **4**, 129–152.

30. J. Marschewski, J. Bin In, D. Poulikakos, and C. P. Grigoropoulos, *Carbon N. Y.*, 2014, **68**, 308–318.

31. L.-M. Lu, L. Zhang, F.-L. Qu, H.-X. Lu, X.-B. Zhang, Z.-S. Wu, S.-Y. Huan, Q.-A. Wang, G.-L. Shen, and R.-Q. Yu, *Biosens. Bioelectron.*, 2009, **25**, 218–223.

32. C. Guo, Y. Wang, Y. Zhao, and C. Xu, *Anal. Methods-UK*, 2013, **5**, 1644-1647.

33. J.-D. Qiu, J. Huang, and R.-P. Liang, *Sensors Actuators B Chem.*, 2011, **160**, 287–294.

34. J.-Y. Chiu, C.-M. Yu, M.-J. Yen, and L.-C. Chen, *Biosens. Bioelectron.*, 2009, **24**, 2015–2020.

35. M. Ammam and E. B. Easton, *Sensors Actuators B Chem.*, 2011, **155**, 340–346.

36. R. Ahmad, M. Vaseem, N. Tripathy, and Y.-B. Hahn, *Anal. Chem.*, 2013, **85**, 10448–10454.

Figure legends

Table 1. Comparison of our sensor with other flexible glucose sensors.

Fig. 1 (A) Schematic illustrations of the fabrication process of Ni-coordinated vertically aligned CNTs on graphite foil (Ni/VCNTs/G). Photographs of (B) flexible Ni/VCNTs/G and (C) various shapes of modified Ni/VCNTs/G.

Fig. 2 SEM image of (A) vertically aligned CNTs (VCNTs/G) and (B) Ni-coordinated vertically aligned CNTs electrode (Ni/VCNTs/G). Energy-dispersive X-ray spectrum of (C) VCNTs/G and (D) Ni/VCNTs/G.

Fig. 3 Cyclic voltammograms of (A) bare graphite foil (a), Ni particles on graphite foil (b), vertically aligned CNTs (VCNTs) (c), Ni-coordinated vertically aligned CNTs electrode (Ni/VCNTs/G) (d) at a scan rate of 50 $mV \cdot s^{-1}$ and (B) Ni/VCNTs/G electrode in 0.1 M NaOH at different scan rates (10 – 200 $mV \cdot s^{-1}$).

Fig. 4 (A) Cyclic voltammograms of Ni-coordinated, vertically aligned CNTs electrode (Ni/VCNTs/G) in 0.1 M NaOH solution with and without 2 mM glucose at scan rate of 50 $mV \cdot s^{-1}$, (B) Amperometric response of Ni-coordinated vertically aligned CNTs electrode (Ni/VCNTs/G) with successive addition of 0.1 mL glucose in 0.1 M NaOH solution at + 0.50 V (inset: amperometric response with addition of 10 and 50 μM) and (b) its corresponding calibration plots before and after 200 bending cycles.

Fig. 5 Amperometric response of Ni-coordinated vertically aligned CNTs electrode (Ni/VCNTs/G) with successive addition of 5.0 mM glucose and 0.1 mM AA, GA, XY, and UA in 0.1 M NaOH solution at + 0.50 V.

Table 1.

Electrode	Potential (V)	Response time (s)	Sensitivity ($\mu A \cdot mM^{-1} \cdot cm^{-2}$)	Linear range (mM)	LOD (μM)	Reference
Ni/VCNTs/G	+ 0.5	2	910.7	0.05 – 1.0	30	Present study
Mn_3O_4 on 3D graphene	+ 0.4	5	360	0.1 – 8	10	9
PtAu-MnO_2 on graphene paper	0	3	58.54	0.1 – 30	20	10
GOx/CS–Fc/GO film	+ 0.3	5	10	0.02 – 6.78	7.6	33
GOx/ZnO nanowires on Au-coated PET	+ 0.8	5	19.5	0.2 – 2.0	50	12
SPCE/CNT/baked PB/PEDOT[GOx] on PET	– 0.1	10	2.67	1.0 – 10	< 100	34
MWCNTs/GOx on PET	+ 0.6	20	5.6	0.02 – 2.2	10	13

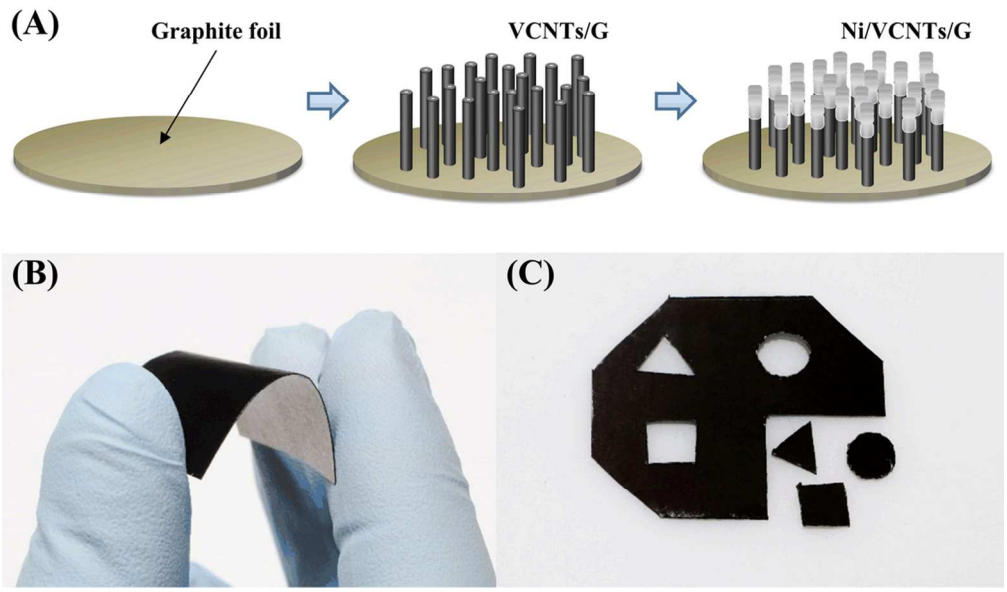

Fig.1 (A) Schematic illustrations of the fabrication process of Ni-coordinated vertically aligned CNTs on graphite foil (Ni/VCNTs/G). Photographs of (B) flexible Ni/VCNTs/G and (C) various shapes of modified Ni/VCNTs/G.
106x62mm (300 x 300 DPI)

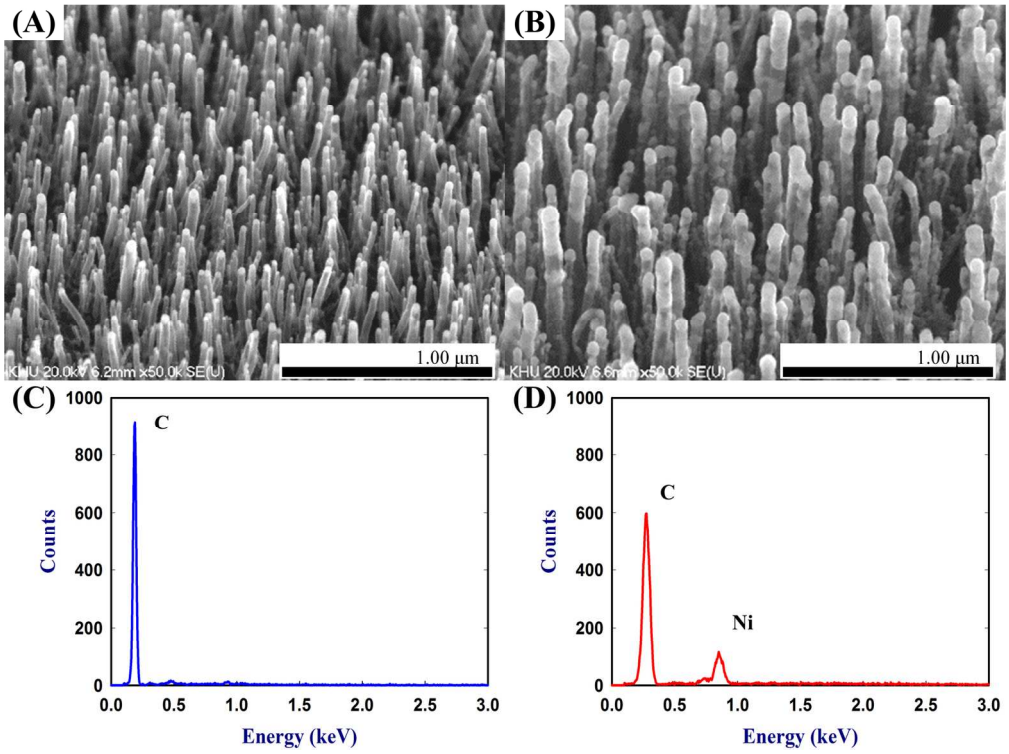

Fig.2 SEM image of (A) vertically aligned CNTs (VCNTs/G) and (B) Ni-coordinated vertically aligned CNTs electrode (Ni/VCNTs/G). Energy-dispersive X-ray spectrum of (C) VCNTs/G and (D) Ni/VCNTs/G.
150x112mm (300 x 300 DPI)

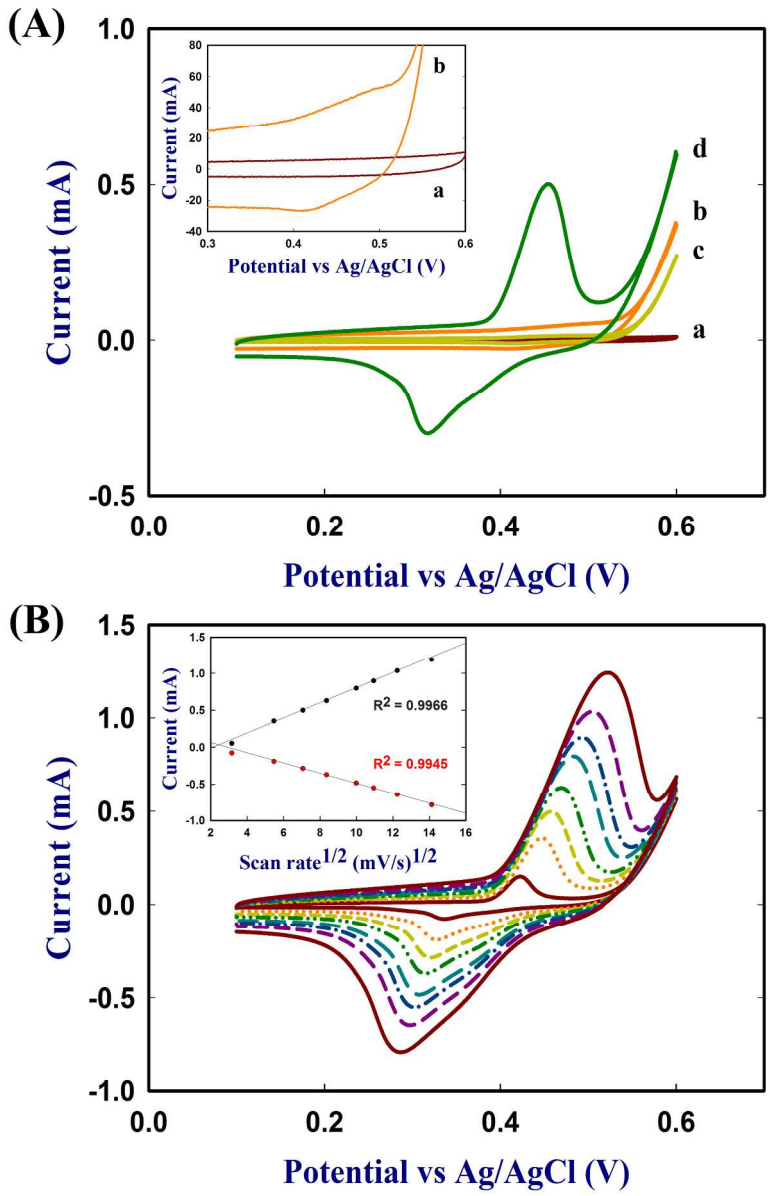

Fig.3 Cyclic voltammograms of (A) bare graphite foil (a), Ni particles on graphite foil (b), vertically aligned CNTs (VCNTs) (c), Ni-coordinated vertically aligned CNTs electrode (Ni/VCNTs/G) (d) at a scan rate of 50 mV•s-1 and (B) Ni/VCNTs/G electrode in 0.1M NaOH at different scan rates (10 – 200 mV•s-1).
181x273mm (300 x 300 DPI)

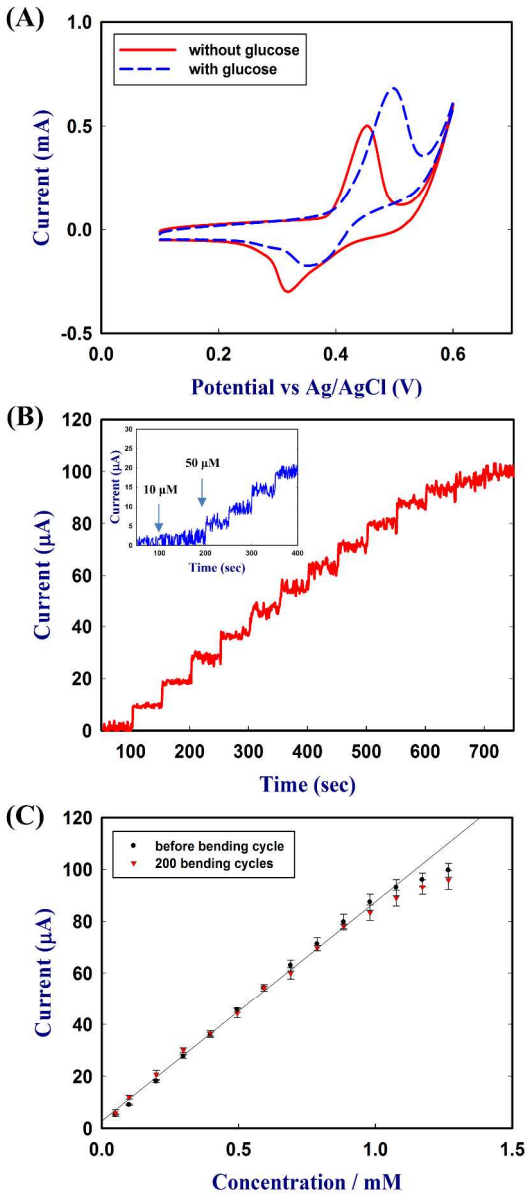

Fig.4 (A) Cyclic voltammograms of Ni-coordinated, vertically aligned CNTs electrode (Ni/VCNTs/G) in 0.1 M NaOH solution with and without 2 mM glucose at scan rate of 50 mV• s-1, (B) Amperometric response of Ni-coordinated vertically aligned CNTs electrode (Ni/VCNTs/G) with successive addition of 0.1 mL glucose in 0.1 M NaOH solution at + 0.50 V (inset: amperometric response with addition of 10 and 50 μM) and (b) its corresponding calibration plots before and after 200 bending cycles.
270x609mm (300 x 300 DPI)

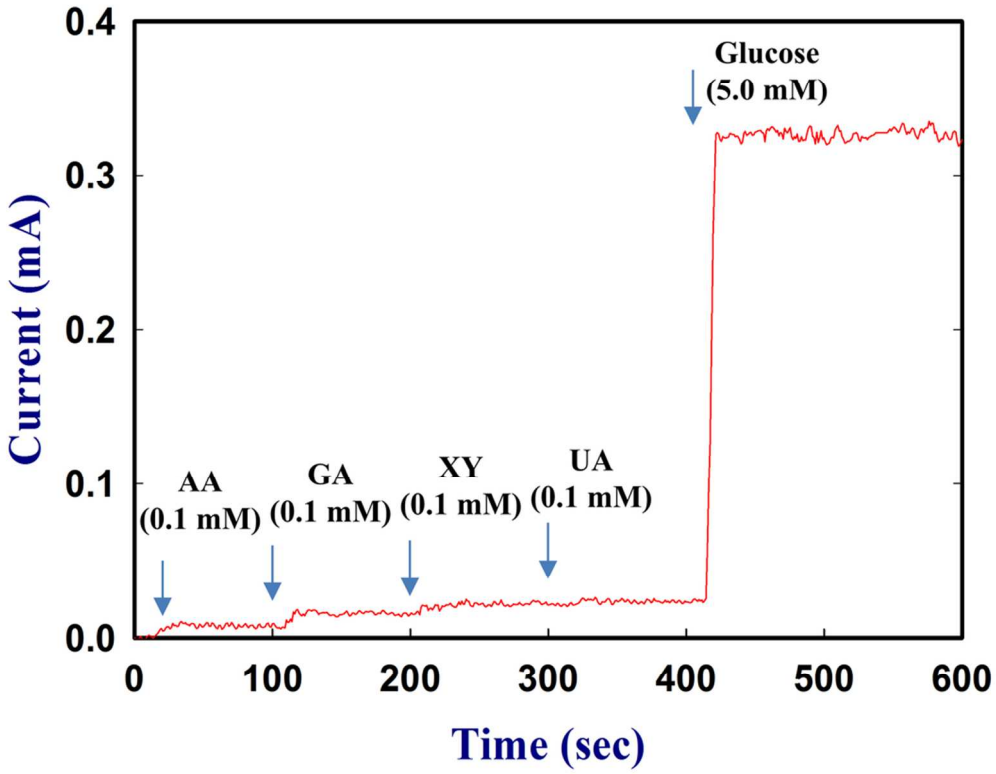

Fig.5 Amperometric response of Ni-coordinated vertically aligned CNTs electrode (Ni/VCNTs/G) with successive addition of 5.0 mM glucose and 0.1 mM AA, GA, XY, and UA in 0.1 M NaOH solution at + 0.50 V.
89x70mm (300 x 300 DPI)